Turbulence Regulation and Stabilization by Equilibrium and Time-Varying, Sheared Turbulence Flows

G.R. McKee,[1] R.J. Fonck,[1] M. Jakubowski,[1] K.H. Burrell, [2] T.N. Carlstrom,[2] C. Fenzi,[1†] R.J. Groebner,[2] K. Hallatschek, [3] R.A. Moyer,[4] W. Nevins,[5] T.L. Rhodes,[6] C. Rost,[7] D. Rudakov,[4] X. Xu[5]

[1]University of Wisconsin-Madison, Madison, Wisconsin 53706 USA,
email: mckee@fusion.gat.com
[2]General Atomics, P.O. Box 85608, San Diego, California 92186-5608 USA
[3]Max-Planck Institut für Plasmasphysik, Garching, Germany
[4]University of California, San Diego, 9500 Gilman Drive, La Jolla, California 92093 USA
[5]Lawrence Livermore National Laboratory, Livermore, California 94551 USA
[6]University of California, Los Angeles, California 90095-1597 USA
[7]Massachusetts Institute of Technology, Cambridge, Massachusetts 02139 USA
[†]Presently with CEA, Cadarache, France

Abstract. Turbulence flows are directly measured in a tokamak plasma by applying time-delay-estimation (TDE) analysis techniques to localized 2-D density fluctuation measurements obtained with Beam Emission Spectroscopy on DIII–D. Time varying, radially localized ($k_\perp * \rho_I < 1$) flows with a semi-coherent structure peaked near 15 KHz and a very long poloidal wavelength, possibly m=0, are observed. These characteristics are very similar to theoretically predicted flows, identified as geodesic acoustic modes, that are self-generated by, and in turn regulate, the turbulence and resulting transport. In addition, the equilibrium radial flow shear near the plasma edge ($0.8 \le r/a \le 1$) varies strongly with magnetic geometry. With the ion ∇B drift directed towards the X–point in a single-null plasma, a large radial shear in the poloidal flow is measured, while much lower shear is observed in the reverse condition. This large shear may thus facilitate the L– to H–mode transition, consistent with the significantly lower L-H transition power threshold in this configuration.

1. Introduction

Turbulent transport, which results from correlated fluctuations in plasma parameters (density, temperature, potential and magnetic field), limits energy confinement in magnetic confinement devices and remains a central scientific challenge to optimizing fusion-energy systems. New fluctuation measurement capabilities, including diagnostics and analysis methods, are providing a more thorough characterization of underlying turbulence behavior. This is allowing for a more quantitative comparison and benchmarking of turbulence simulations and explaining global plasma behavior. Here, we present direct measurements of the equilibrium and time-varying flow field of turbulent eddies and their potential effects on the turbulence and resulting transport.

Measurements of turbulence flows are obtained with 2-D density fluctuation data obtained with the DIII–D beam emission spectroscopy (BES) system [1]. 32 viewing channels are available and have been deployed to obtain 2-D measurements [2,3] over a roughly 5 cm (radial) × 6 cm (poloidal) spatial region at the outboard tokamak midplane (5 × 6 channel grid). Figure 1 illustrates the typical arrangement of spatial channels relative to the magnetic equilibrium. The array can be scanned radially on a shot-to-shot basis to obtain detailed profile information.

The relevant turbulence flows, which are the group velocity of the turbulent eddies, and should be distinguished from bulk mass flow, are dominantly in the poloidal direction. They range in frequency from nearly steady-state up to the decorrelation rates for long wavelength density turbulence (f > 100 kHz). Equilibrium measurements of flow are obtained using time-delay correlation analysis between adjacent spatial channels [4]. The measurement of high-frequency turbulence flows has required the development of specialized time-delay-estimation (TDE) techniques and application of these techniques to the localized density fluctuation measurements. One method utilizes wavelet-based time-delay correlations to provide measurements at a frequency up to almost the upper-frequency limit of the density spectrum itself [5]. A second technique utilizes time-resolved cross-correlation analysis, and can obtain resolutions of up to about 20 μs [6,3].

2. Self-Regulating Turbulence Flows

Time-varying poloidal flows that exhibit spatial and temporal characteristics of theoretically-predicted axisymmetric sheared flows have been measured by applying TDE analysis to 2-D BES fluctuation data. Turbulence theory and simulations predict the existence of self-generated axisymmetric (n=0) flows that act to regulate the turbulence amplitude. These flows exhibit a low-frequency branch, often referred to as zonal flows [7–9], and a related higher frequency component, identified as geodesic acoustic modes (GAM) [10]. Zonal flows and GAMs, predicted to be toroidally and azimuthally symmetric electrostatic potential structures (m=n=0) with narrow radial extent ($k_\perp \rho_I < 1$), regulate turbulence through the time-varying $E_r \times B_T$ flows. As such, these flows are expected to be manifest in the poloidal flow-field of the density fluctuations. Initial observations that imply the existence of such flows have been obtained from measurements of edge density and potential fluctuations [11–15].

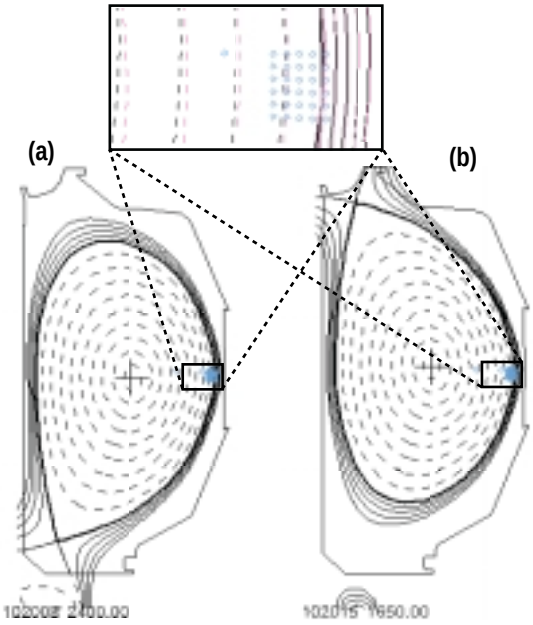

Fig. 1. Magnetic equilibrium and 2-D BES viewing geometry (inset) for turbulence flow measurements near the outer midplane: (a) lower single-null (ion ∇B towards X–point), (b) upper single-null (ion ∇B away from X–point).

Time-dependent poloidal velocity measurements are obtained with the TDE techniques discussed above. Spectral analysis of the resulting $v_\theta(t)$ measurement is shown in Fig. 2. The v_θ spectrum exhibits a coherent oscillation near 15 kHz superimposed on a broadband feature. The mode flow amplitude is approximately 10% of the equilibrium poloidal flow of turbulence, which itself is typically comparable to the $E_r \times B_T$ velocity. The coherent 15 kHz oscillation is not associated with any MHD activity.

Figure 3 shows the measured phase shift of the v_θ oscillation across the measured region. Poloidally, the 15 kHz v_θ structure shows little or no measurable phase shift, suggesting a long-wavelength, low-m structure. The limited poloidal extent of the measurements and their respective uncertainty suggests $|m|<3$ if a uniform poloidal perturbation is assumed. Radially, the flow structure exhibits a rapid phase shift, undergoing a full 180° change over about 3 cm. This radially-sheared flow could be capable of shearing turbulent eddies, given sufficient

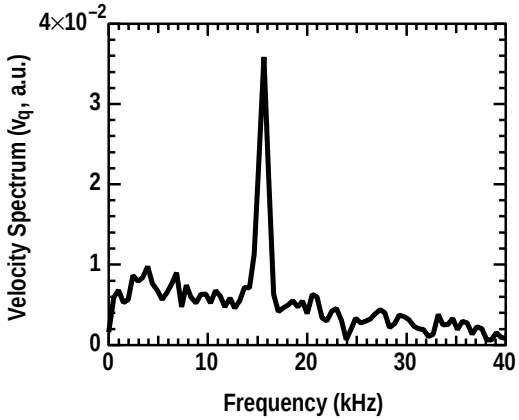

Fig. 2. Poloidal velocity cross-power spectrum at r/a=0.95 exhibiting coherent flow oscillation near 15.5 kHz.

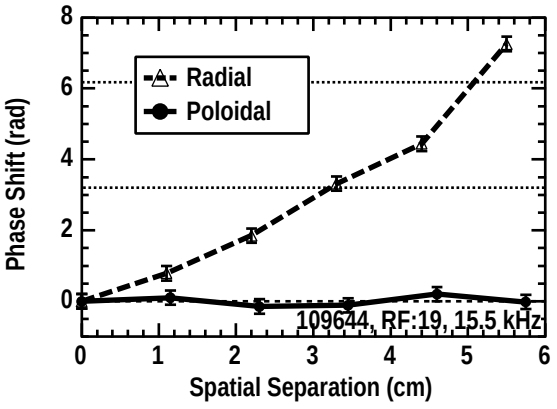

Fig. 3. Radial and poloidal phase relationship of coherent v_θ oscillation at 15.5 kHz.

amplitude and sufficiently low frequency [16,17]. Estimates of the shearing rate have been derived from the measured amplitude and spatial structure. They are comparable to, though somewhat less than, the decorrelation rate of the turbulence, qualitatively indicating that the flow is of sufficient amplitude to mediate the turbulence amplitude [18].

Simulations of turbulence in the edge-to-core transitional regime [10] predict that the frequency of GAMs depends on temperature. To test this prediction, and examine whether the observed poloidal flow oscillations might be GAMs, the temperature was varied during a series of discharges by adjusting the input power. The frequency of this coherent poloidal flow oscillation is indeed shown to depend on the plasma temperature in a fashion consistent with these predictions.

Figure 4 shows the poloidal velocity spectra from two discharges, measured at the same spatial location and discharge time, but with different local temperatures. The mode frequency increases from about 13 to 16 kHz as the local electron T_e is increased from 65 to 90 eV. A monotonic dependence on temperature is observed, consistent with the hypothesis that the observed mode is a geodesic acoustic mode. GAM frequencies are predicted to scale with the sound speed, and thus temperature, as $f_{GAM} \approx c_s/2\pi R_{major}$. Calculating this frequency for these discharges with $C_s = \sqrt{(T_e + T_i)/M_I}$ yields f_{GAM} =13 kHz, very close to the observed frequency. The predicted frequency also depends on terms of order unity that depend on the exact magnetic geometry.

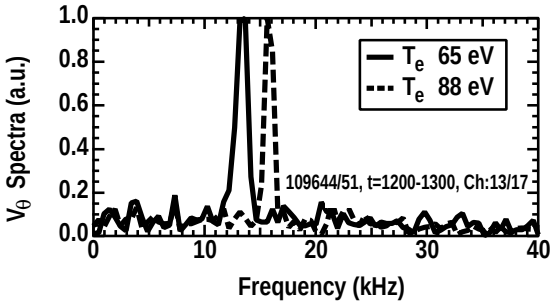

Fig. 4. (a) v_θ spectra at r/a=0.95 in plasmas with different electron temperature and plasma.

A small but measurable density fluctuation is observed to be correlated with the poloidal flow oscillation. These density fluctuations have a relatively small amplitude, $\tilde{n}/n \sim 0.25\%$. In contrast to the poloidal flow oscillation, the density fluctuation exhibits a finite phase shift in the poloidal direction, as well as in the radial direction. Assuming a uniform poloidal perturbation, extrapolating the measured phase shift (over 6 cm) around the poloidal extent of the tokamak plasma yields $m \approx 10$. This is significantly higher than the theoretically predicted value. GAMs are predicted to result from a coupling of an m/n=1/0 pressure perturbation to the toroidal magnetic geometry. This will need to be reconciled with relevant theory.

3. Dependence of Turbulence flow on Magnetic Geometry

The power threshold required to induce the L–mode to H–mode transition in tokamaks has been shown to be highly dependent on the magnetic geometry of the divertor. Plasmas having the ion ∇B drift pointing towards the X–point (lower single-null, LSN) exhibit a 2–3 times lower H–mode power threshold relative to plasmas with the ion ∇B drift pointing away from the X–point (upper single-null, USN) [19]. The physical mechanism responsible for this large difference in power threshold has not been experimentally identified, yet is of great relevance to understanding L– to H–mode transition dynamics. Basic plasma parameter profiles (density, temperature, rotation) are similar near the edge in these two plasma configurations in L–mode at constant input power [19]. The magnetic geometry for both configurations was shown in Fig. 1.

Detailed fluctuation characteristics have been measured near the outer midplane in these two plasma configurations. Several characteristics of the turbulence differ dramatically in these two configurations in a manner that may explain the large L-H transition power threshold differences.

The poloidal dispersion relation (k_θ versus ω) of the turbulence at r/a=0.9 for the LSN and USN configurations is compared in Fig. 5. Each data point is analyzed by frequency filtering

the fluctuation data and calculating the corresponding $S(k_\theta)$ wavenumber spectra using six poloidally-separated channels in the 2-D array [20]. The dramatic difference in the dispersion is apparent, with the USN plasma exhibiting a monotonically increasing wavenumber with frequency out to near 120 kHz. This direction corresponds to the ion diamagnetic direction in the laboratory frame. The LSN plasma, in contrast, exhibits wave propagation directed in the opposite direction (electron diamagnetic direction) and a lower frequency range, only extending up to near 75 kHz. The LSN turbulence also exhibits a dual-mode nature, with the lowest frequency turbulence (f<8 kHz) convecting in the ion direction. This indicates the presence of counter-propagating modes at the same radial location, a phenomenon that was also reported in TFTR plasmas [21].

A comparison of the equilibrium poloidal turbulence flows is shown in Fig. 6. This shows the poloidal group velocity of the turbulence evaluated using time-delay correlation analysis. Where double modes exist in the LSN plasma, the dominant (higher frequency) band has been evaluated. Plasmas with the ion ∇B drift pointing towards the dominant X–point (LSN) exhibit a sharp reversal of the eddy poloidal flow direction near r/a ≈ 0.92 ($R-R_{sep}$ = –3 cm). Inboard flow in both cases convects in the same (ion diamagnetic) direction at nearly the same velocity, the direction expected from the beam-induced E×B rotation. This results in a large radial shear in the poloidal turbulence flow for the LSN configuration. No such flow reversal is observed in the USN plasma.

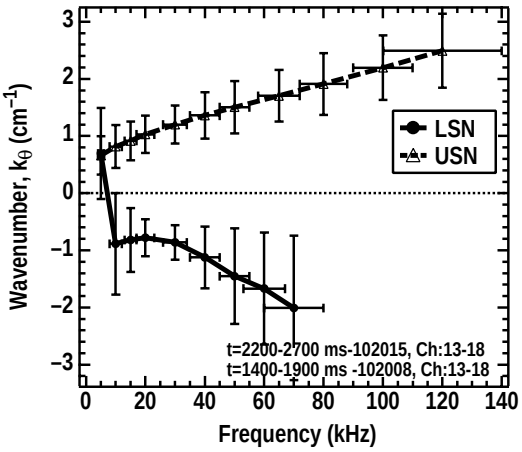

Fig. 5. Poloidal dispersion relation of turbulence near r/a=0.92 for USN and LSN plasmas. Horizontal bars indicate frequency band for given data point, and vertical bar represents FWHM of calculated $S(k_\theta)$ wavenumber spectrum.

The radial correlation functions of the turbulence for the two configurations are compared in Fig. 7. The correlation length, taken as the 1/e point, is reduced from 1.8 cm in the USN case to 1.15 cm in the LSN case. For the USN case, the correlation is integrated over a wide frequency band (15–200 kHz), while for the LSN case, the correlation is integrated over the higher frequency mode (of the two observed modes) since this is the frequency band that undergoes the flow reversal. This is consistent with the notion that the turbulence flow shear may be acting to reduce the average radial extent of the turbulent eddies in this flow shear region.

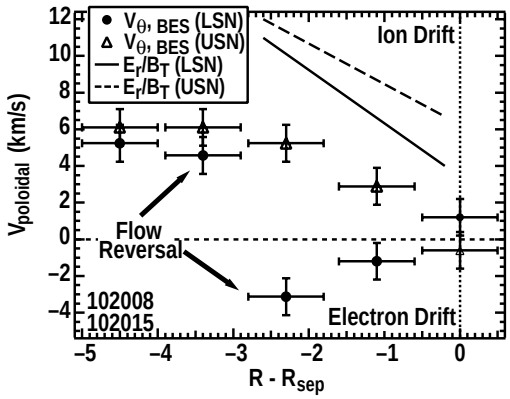

Fig. 6. Poloidal group velocity profile of density turbulence in USN and LSN conditions evaluated from time-delay correlation analysis, and a comparison to the measured E×B velocities from charge exchange recombination spectroscopy.

The effective shearing rate resulting from the flow profile in Fig. 7 can be qualitatively estimated as $\omega_s = dv_\theta/dr \approx 8\times10^5\ s^{-1}$. This can be compared to the locally measured nonlinear decorrelation rate of the turbulence, $\gamma_c \approx 1/\tau_c \approx 10^5\ s^1$, and so $\omega_s > \gamma_c$. Thus, the turbulence flow shear appears to be of sufficient magnitude to affect the turbulence and perhaps facilitate the L-H transition [16]. We note that in this case, the shear is observed in the turbulence flow itself rather than in the E×B shear which is comparable in the two configurations and does not exhibit a change in sign, as shown in Fig. 6.

We thus speculate that this naturally occurring shear condition, apparent in plasmas with the ion ∇B drift direction pointing towards the X–point (LSN), may facilitate the L– to H–mode transition. Furthermore, this may explain the dramatically lower power threshold in these plasmas compared with those with the ion ∇B drift pointing away from the X–point (USN). These results are consistent with recent BOUT simulations [22] also showing a flow reversal in similar plasmas, though further study is required.

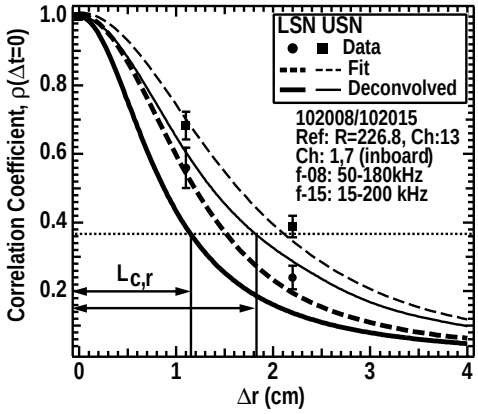

Fig. 7. Comparison of radial correlation functions of density fluctuations for USN and LSN. Correlation is measured inward from reference channel at r/a=0.95. Dashed lines indicate fits to data points, and solid lines indicate correlation after deconvolution of finite spatial resolution.

Acknowledgment

Work supported by U.S. Department of Energy under Grants DE-FG03-96ER54373, DE-FG03-95ER-54294, DE-FG03-01ER54615, DE-FG02-94ER54235, and Contracts DE-AC03-99ER54463, and W-7405-ENG-48.

References

[1] G. McKee *et al.*, Rev. Sci. Instrum. **70**, 913 (1999).
[2] C. Fenzi, *et al*., Rev. Sci. Instrum. **72**, 968 (2001).
[3] G. McKee *et al.*, *accepted* Rev. Sci. Instrum. (2003).
[4] R.D. Durst, R.J. Fonck, G. Cosby, H. Evensen, Rev. Sci. Instrum. **63** (10), 4907 (1992).
[5] M. Jakubowski *et al.*, Rev. Sci. Instrum.**72**, 996 (2001).
[6] H.C. So, Electron. Lett. **34**, 722 (1998)
[7] P.H. Diamond *et al.*, Proceedings of the 17th IAEA Fusion Energy Conference, Report No. IAEA-CN-69/TH3/1, 1998.
[8] T.S. Hahm *et al.*, Plasma Phys. Control. Fusion **42**, A205 (2000).
[9] Z. Lin *et al*., Science **281**, 1835 (1998).
[10] K. Hallatschek *et al.*, Phys. Rev. Lett. **86**, 1223 (2001).
[11] S. Coda S, M. Porkolab, K. H. Burrell, Phys. Rev. Lett. **86**, 4835 (2001).
[12] G.R. Tynan *et al.*, Phys. Plasmas **8**, 2691 (2001).
[13] R.A. Moyer *et al*., Phys. Rev. Let. **87**, 135001 (2001).
[14] Y.H. Xu *et al*., Phys. Rev. Let. **84**, 3867 (2000).
[15] M.G. Shats, W. M. Solomon, Phys. Rev. Let. **88**, 045001 (2002).
[16] K.H. Burrell, Science **281**, 1816 (1998).
[17] P.W. Terry, Rev. Mod. Phys. **72**, 109 (2000).
[18] M. Jakubowski, R. Fonck, G. McKee, submitted to Phys. Rev. Lett. (2002).
[19] T. Carlstrom *et al.*, Plasma Phys. Control. Fusion **44** 1 (2002).
[20] R.J. Fonck, et al., Phys. Rev. Let. **70**, 3736 (1993).
[21] R. Durst, R.J. Fonck, J.S. Kim *et al.*, Phys. Rev. Lett. **71**, 3135 (1993).
[22] X. Xu *et al.*, Phys. Plasmas **7**, 1951 (2000).